

AN ANALYSIS OF KEROGEN DISTRIBUTION IN GREEN RIVER OIL SHALE

John F. Patzer, II

Chemicals and Minerals Division
Gulf Research & Development Company
Pittsburgh, Pennsylvania 15230

ABSTRACT

The classification of Green River oil shales through density separation techniques reveals some new insights into the naturally occurring distribution of kerogen in shale. Twelve Colorado shales and one Utah shale, covering a range of sources and grades, were classified into fractions of varying kerogen content through heavy-media density separation. Analysis of the separation data reveals that the shales all have a linear relationship between the enriched grade kerogen content and the weight fraction of total kerogen recovered in the enriched grade. The slope of the linear relationship correlates with the original shale kerogen content. The correlation provides a powerful tool for a priori prediction of the results for any classification process which operates on density separation. The existence of such a linear relationship implies that the naturally occurring differential mass distribution function for kerogen in shale is an inverse relation between weight fraction of shale and kerogen content of the fraction, i.e., kerogen-lean fractions are present in much greater quantity than kerogen-rich fractions. Another aspect of the distribution function is the existence of clearly defined, sharp cut-points which contain the entire distribution within a range of kerogen content dependent upon the original shale grade.

The Green River oil shale formation comprises one of the largest fossil fuel energy reserves in the world. Commercial development of this source is very likely to become a reality within the next five to ten years. Initial development will almost certainly use current retorting technology. However, full scale development will probably occur only after second generation technology, now in development in many research labs, reaches commercial viability. Knowledge and understanding about how kerogen is distributed within the shale formation will aid in developing more selective, viable processes for recovery of the energy contained in the kerogen.

Gulf has been interested for several years in the potential possibility of selectively discarding very lean shales prior to retorting. If the economic cost of such selective rejection were low enough, the reduction in shale volume retorted for equivalent oil production could yield potential benefits through lowered capital and operating costs for a retort and, possibly, through lessened environmental impact because less shale would be processed.

The correlation between shale density and Fischer Assay yield has been known for many years.^{1,2} Figure 1, due to Smith,¹ shows the expected Fischer Assay as a function of density. The existence of such a correlation results from the wide separation between kerogen and mineral matter density in shale, about 1070 kg/m³ and 2720 kg/m³, respectively, and the narrowness of the mineral matter density range. Smith² developed the relations

$$(GPT) = (31.563 \cdot 10^{-6}) (D_T)^2 - 0.205998 (D_T) + 326.624 \quad (1)$$

$$x_w^o = \frac{D_o}{D_m - D_o} \left(\frac{D_s}{D_T} - 1 \right), \quad (2)$$

$$x_w^m = 1 - x_w^o = \frac{D_m}{D_m - D_o} \left(1 - \frac{D_o}{D_T} \right), \quad (3)$$

$$x_V^O = \frac{1}{D_m - D_o} (D_m - D_T), \quad (4)$$

$$x_V^m = 1 - x_V^O = \frac{1}{D_m - D_o} (D_T - D_o), \quad (5)$$

to describe the interrelationships between the shale density and shale organic content. Equation (1) is the least-squares representation of the correlation shown in Figure 1. Equations (2) to (5) are derived from simple material balance considerations. A best fit to numerous data requires the mineral matter density, $D_m = 2720 \text{ kg/m}^3$, and the organic density, $D_o = 1050$ to 1070 kg/m^3 .

Heavy-Media Separation

The relation between density and organic content provides the basis for a separations scheme based upon density differences.^{3,4} Twelve Colorado shales and one Utah shale, as shown in Table 1, were separated by heavy-media techniques at the Institute of Mineral Research, Michigan Technological University. The shales represent a variety of grades, ranging from 16.5 to 44.2 GPT, and a variety of particle sizes.

The separations were performed in both batch and continuous circuit operations as schematically depicted in Figure 2. The shale sample was immersed in a bath of given density and separated into sink-and-float fractions. The sink fraction was collected. The float fraction was immersed in a bath of lower density and split into sink-and-float fractions. The procedure was performed at least twice, and as many as five times, on the various shales. An air pycnometer was used to determine the density of each separate fraction produced by the sink/float operation. The original sample density was then back-calculated from the individual fraction densities. The heavy-media separations experiments provide cumulative weight fraction distribution curves as a function of specific gravity, as depicted in Figure 3 for shales D

and I. The relatively lean shale D and relatively rich shale I have distinctly different cumulative distribution curves. As is expected from the relation between Fischer Assay and density, the richer shale contains considerably more lower density material than the leaner shale.

The heavy-media separations were analyzed on the basis of splitting the original sample into two fractions, a rich shale fraction and a lean shale fraction, as depicted in Figure 4. The weight fraction organic, (X_w^0) , for each split was determined by calculating the density of each split and using Equation (2).

A measure of the efficiency of the separation process, i.e., the ability to selectively separate rich from lean shales, is obtained by plotting $(X_w^0)_1$, versus the organic recovery in the rich fraction,

$$R = (X_w^0)_1 (w_1) / (\bar{X}_w^0), \quad (6)$$

as shown in Figure 5. An enrichment plot, such as Figure 5, is a concise statement about the ability to perform a separation and the economic benefit of doing so. When the separations operating parameter, in this case, density, is a continuous variable, it is possible to draw a continuous performance curve which describes the separations potential for the mineral. The shape and properties of the performance curve will be determined solely by the distribution of the variable under consideration. Clearly, a very steep slope in the $R > 0.90$ range is desirable for a truly efficient separation process.

The results of the heavy-media separation experiments are shown in Figure 6. Four separate panels are shown only for clarity. The experimental data points are indicated by open symbols. The lines are the result of linear least-squares regression of the data. The most remarkable feature of Figure 6 is that all of the data can be adequately represented by the linear representation

$$(X_w^0)_1 = mR + b \quad (7)$$

Table II provides the calculated values for the slopes and the correlation coefficient for the regression. The goodness of the linear fit is indicated by the range of correlation coefficients, 0.95 to 0.99.

The ability to make an a priori prediction of the slope based only upon knowledge of the feed shale organic concentration, or equivalently, density, would allow prediction of heavy-media separation results. It would also provide a method for heavy-media process control. Figure 7 shows a relation between the slope and feed shale weight fraction organic, given by

$$m = 0.671 - 10.21 (\bar{x}_w^0) + 28.423 (\bar{x}_w^0)^2 \quad (8)$$

The equation, obtained from a quadratic least-squares regression, is only a marginal fit to the data. However, it provides a reasonable estimate for engineering purposes.

With a priori knowledge of the slope, it is possible to predict density separations results. The intercept, b , is obtained from

$$b = (\bar{x}_w^0 - m) \quad \text{at } R = 1 \quad (9)$$

Figure 8 depicts a comparison between the actual and predicted separations results for shales D and I. The linear fit correlation using the coefficients predicted by (8) and (9) reproduce the experimental least-squares relations within an average error of 9% and a maximum deviation of 19%. Thus, it is possible to make reasonable a priori predictions of heavy-media results.

Kerogen Distribution in Shale

The linear relation between weight fraction organic in the enriched shale and kerogen recovery can be used to obtain some basic information about the distribution of kerogen in oil shale. Assuming that the weight fraction

organic can be represented as a continuous variable, a differential weight fraction distribution function can be defined by

$$\int_{\tilde{X}_w^0}^{\tilde{X}_w^0} f(\tilde{X}_w^0) d\tilde{X}_w^0 = 1 \quad (\text{normalization}) \quad (10)$$

$$\int_{\tilde{X}_w^0}^{\tilde{X}_w^0} \tilde{X}_w^0 f(\tilde{X}_w^0) d\tilde{X}_w^0 = \tilde{X}_w^0 \quad (\text{expected value}) \quad (11)$$

where $f(\tilde{X}_w^0) d\tilde{X}_w^0$ represents the differential shale mass between organic content \tilde{X}_w^0 and $\tilde{X}_w^0 + d\tilde{X}_w^0$. The upper limit on \tilde{X}_w^0 is readily obtainable from the linear relation (7) as $(\tilde{X}_w^0)_{\max} = b$ at $R = 0$.

The functional form of the differential shale mass distribution function can be obtained by back-calculating f_j as a function of $(\tilde{X}_w^0)_i$ from (7) by incrementing R in even steps, as

$$(\tilde{X}_w^0)_{1,i} = mR_i + b = \frac{\sum_{j=1}^i f_j (\tilde{X}_w^0)_j}{\sum_{j=1}^i f_j} \quad (12)$$

$$w_{1,i} = \frac{R_i (\tilde{X}_w^0)_i}{(\tilde{X}_w^0)_{1,i}} = \frac{i}{\sum_{j=1}^i f_j} \quad (13)$$

to obtain

$$f_j = w_{1,i} - \sum_{j=1}^{i-1} f_j \quad (14)$$

$$(\bar{X}_w^0)_i = \frac{(\bar{X}_w^0)_{1,i} w_{1,i} - \sum_{j=1}^{i-1} f_j (\bar{X}_w^0)_j}{f_i} \quad (15)$$

The average kerogen concentration of the sample, (\bar{X}_w^0) , is a known and the values of m and b are prescribed through the linear correlation. In the limit as $i \rightarrow \infty$, one obtains the continuous differential shale mass distribution function

$$f(\bar{X}_w^0) = A/(\bar{X}_w^0) \quad (16)$$

by this procedure.

The final two unknowns for the differential distribution function, A and $(\bar{X}_w^0)_{\min}$, are obtained through application of the normalization and expected value properties of the distribution function,

$$\int_{(\bar{X}_w^0)_{\min}}^{(\bar{X}_w^0)_{\max}} f(\bar{X}_w^0) d\bar{X}_w^0 = A \ln [(\bar{X}_w^0)_{\max} / (\bar{X}_w^0)_{\min}] = 1 \quad (17)$$

$$\int_{(\bar{X}_w^0)_{\min}}^{(\bar{X}_w^0)_{\max}} (\bar{X}_w^0) f(\bar{X}_w^0) d\bar{X}_w^0 = A [(\bar{X}_w^0)_{\max} - (\bar{X}_w^0)_{\min}] = \bar{X}_w^0 \quad (18)$$

Note that the normalization property implies that there also exists a practicable minimum naturally occurring grade of shale present in any given deposit. Figure 9 shows the differential weight fraction distribution function for 20 GPT and 35 GPT shales based upon the predictive correlation of

equations (8) and (9). Although Figure 9 shows very sharp cut-off points in the distribution, naturally occurring distributions are likely to have some tailing effects.

Although a straight-line relation between weight fraction kerogen content and weight fraction kerogen recovery has the unique representation in differential shale mass distribution function space given by Equation (16), the actual distribution of kerogen in shale might differ somewhat from the inverse proportional relationship. This results because the straight-line relation is an inference from least-squares regression of the data and because the least-squares regressions are not perfect, i.e., correlation coefficient equal to one. In order to validate the differential distribution function, it is important to examine the cumulative weight fraction data of the heavy-media separations experiments in differential manner. Because of the small number of data points available per sample, such differential distributions are only crude representations of the actual distribution.

Figure 10 presents the histogram of weight fraction kerogen for shale D normalized so that the area under the bars equals one. Such a histogram is an approximation to the differential distribution function. The plotted histogram is similar to the derived inverse proportional distribution function. However, some tailing which is evident at the leaner grades of shale indicates that a rival distribution function, the log normal distribution function given by

$$f(\tilde{x}_w^0) = \frac{1}{\sqrt{2\pi} \sigma} \cdot \frac{1}{(\tilde{x}_w^0)} \exp \left[\frac{-(\ln \tilde{x}_w^0 - \xi)^2}{2\sigma^2} \right] \quad (19)$$

could also approximate the distribution.

The inverse proportional distribution function is described by the parameters A, $(\tilde{x}_w^0)_{\max}$ and $(\tilde{x}_w^0)_{\min}$ which are directly determinable and related in a fundamental, physical manner to the shale. The log normal distribution has two parameters, ξ and σ which have no readily determinable

physical relation to shale. They can be determined in a reasonable manner, however, by assuming that 95% of the shale has kerogen content less than the $(\bar{X}_w^0)_{\max}$ predicted by the a priori method, Equations (7), (8) and (9). Figure 11 contrasts the predicted inverse proportional and log normal differential distribution functions for a 20.6 GPT shale. The two distributions are similar, with rapid rise to a maximum in kerogen content and tailing off toward richer shales. The log normal distribution is more diffuse, with greater tailing at both the rich and lean ends of the distribution.

Figure 12 shows the predicted enrichment plot for a 20.6 GPT shale with the inverse proportional and log normal differential distribution functions as parameters. A heavy vertical bar is drawn at $R=0.20$ to emphasize that this was the smallest value on the abscissa which was obtained in the experimental study. The salient feature of Figure 12 is that for values of $R < 0.20$, both distributions could easily give least-squares representations as straight lines; significant curvature in the log normal distribution occurs at values of $R < 0.20$. Thus, it is doubtful that the experimental data can readily distinguish between the two distributions.

The inverse proportional distribution is, however, the recommended distribution function for describing a shale resource for three reasons. First, the parameters which define the distribution have real, physical meaning which readily define what is present in a shale deposit. Second, the functional form of the inverse proportional distribution is more easily worked with in analytical equations than is the functional form of the log normal distribution. Finally as demonstrated in Figure 13, the inverse proportional distribution function provides excellent agreement with experimental observations.

ACKNOWLEDGMENT

The author is indebted to O. A. Larson of GR&DC who conceived of and directed the experimental program which provided the data necessary for this analysis and to C. W. Schultz and E. L. Michaels who performed the experiments at the Institute of Mineral Research, Michigan Technological University.

NOMENCLATURE

b	intercept in linear relation
D_o	kerogen (organic) density, kg/m^3
D_m	mineral density, kg/m^3
D_T	oil shale density, kg/m^3
GPT	oil shale Fischer Assay, gal/ton
m	slope in linear relation
R	weight fraction organic recovery
x_v^o	volume fraction kerogen (organic) in shale
x_v^m	volume fraction mineral in shale
x_w^o	weight fraction kerogen (organic) in shale
x_w^m	weight fraction mineral in shale
\bar{x}_w^o	average weight fraction kerogen (organic)
\tilde{x}_w^o	point weight fraction kerogen (organic)
w	weight fraction of shale

subscripts

1	riched fraction from heavy-media separation
2	lean fraction from heavy-media separation
i	increment index
j	increment index

REFERENCES

1. Smith, John Ward, "Specific Gravity-Oil Yield Relationship of Two Colorado Oil Shale Cores," Ind. Eng. Chem., 48 (3), 441 (1956).
2. Smith, John Ward, "Theoretical Relationship Between Density and Oil Yield for Oil Shales," USBM ROI 7248, 1976.
3. O. A. Larson, to appear in ACS Symposium Series.
4. J. F. Patzer, manuscript submitted to Fuel.

TABLE I
OIL SHALES USED FOR HEAVY MEDIA SEPARATION

<u>SHALE</u>	<u>GPT</u>	<u>SIZE, CM</u>	<u>SOURCE</u>
A	16.5	0.20-0.64	C-8 TRACT, MAHOGANY ZONE
B	19.2	0.64-5.08	ANVIL POINTS MINE, 0 TO +20 FT, MAHOGANY MARKER
C	19.3	0.64-5.08	C-8 TRACT, MAHOGANY ZONE
D	22.0	0.64-7.62	RIFLE MINE, COMPOSITE BEDS A, B, C, E, F, G, H, I, J
E	22.2	0.64-1.91	RIFLE MINE, COMPOSITE BEDS A, B, C, E, F, G, H, I, J
F	22.6	0.64-7.62	RIFLE MINE, BEDS A, B, C
G	26.7	0.64-5.08	ANVIL POINTS MINE, -20 TO -40 FT, MAHOGANY MARKER
H	29.8	0.64-7.62	RIFLE MINE, BEDS E, F
I	30.9	0.64-5.08	ANVIL POINTS MINE, 0 TO -20 FT, MAHOGANY MARKER
J	32.1	0.64-7.62	RIFLE MINE, BEDS G, H, I, J
K	36.1	0.64-5.08	HELL'S COLE CANYON, UTAH, MAHOGANY ZONE
L	38.7	0.64-15.2	HORSE DRAW CREEK, R-3 ZONE, USBM 96" SHAFT
M	44.2	0.64-15.2	HORSE DRAW CREEK, R-4 ZONE, USBM 96" SHAFT

TABLE II

LINEAR REGRESSION OF HEAVY MEDIA SEPARATION RESULTS

$$(X_{W1}^0)_1 = mR + b$$

<u>SHALE</u>	<u>SLOPE, m</u>	<u>CORRELATION COEFFICIENT</u>
A	-0.116	-1.000
B	-0.157	-0.977
C	-0.083	-0.995
D	-0.174	-0.995
E	-0.151	-0.997
F	-0.105	-0.997
G	-0.250	-0.996
H	-0.274	-0.987
I	-0.301	-0.969
J	-0.268	-0.982
K	-0.262	-0.993
L	-0.083	-0.949
M	-0.132	-0.986

Figure 1

SHALE GRADE AS A FUNCTION OF DENSITY

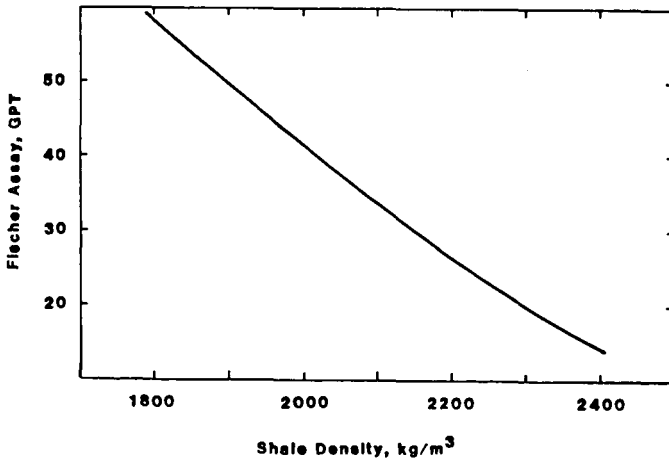


Figure 2
HEAVY MEDIA OIL SHALE SEPARATIONS

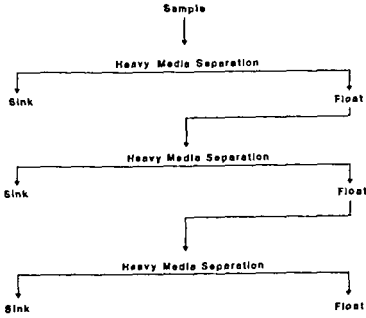


Figure 4
OIL SHALE BENEFICIATION ANALYSIS

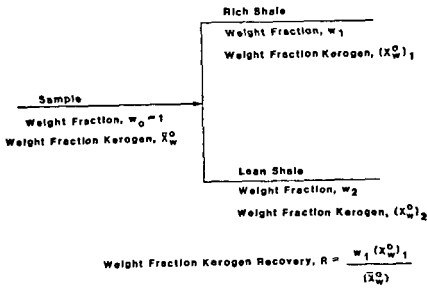


Figure 3
CUMULATIVE WEIGHT FRACTION DISTRIBUTION CURVE FOR HEAVY-MEDIA SEPARATION OF OIL SHALE AS A FUNCTION OF SPECIFIC GRAVITY

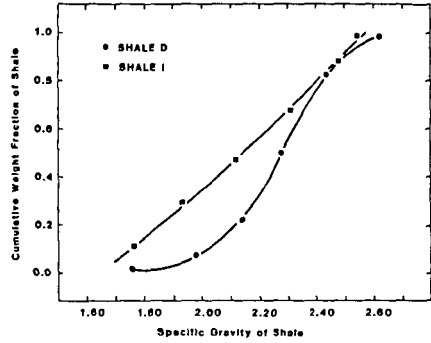


Figure 5
TYPICAL ENRICHMENT PLOT FOR OIL SHALE BENEFICIATION

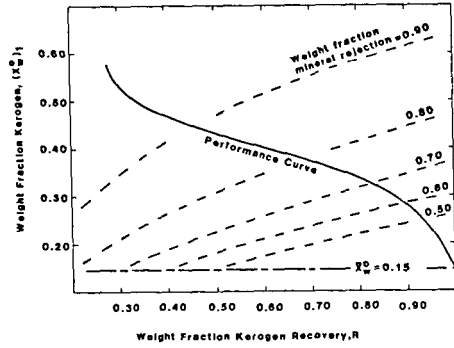


Figure 6
HEAVY MEDIA SEPARATIONS RESULTS

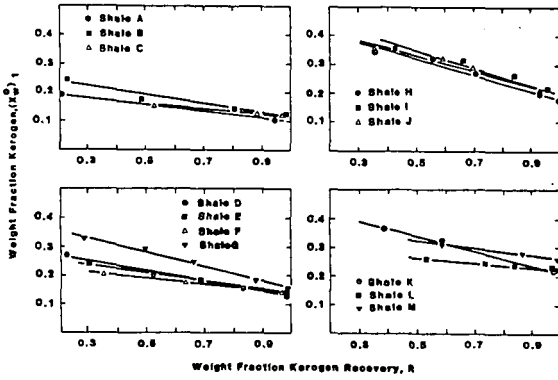


Figure 7
SLOPE OF LINEAR BENEFICIATION EQUATION
AS A FUNCTION OF FEED SHALE KERODEN CONTENT

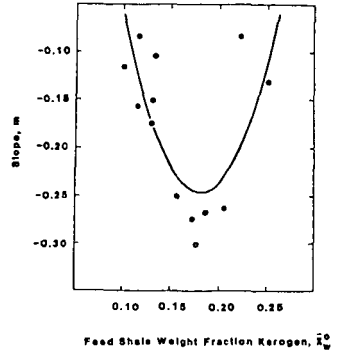


Figure 8
COMPARISON BETWEEN ACTUAL AND PREDICTED RESULTS
FOR HEAVY MEDIA SEPARATION OF SHALE

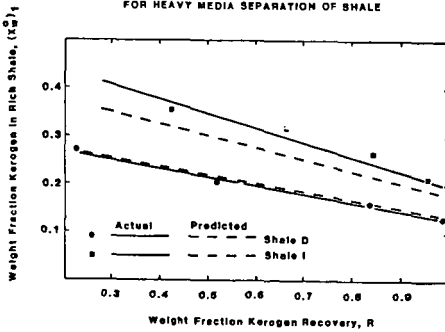


Figure 9
DIFFERENTIAL DISTRIBUTION FUNCTION

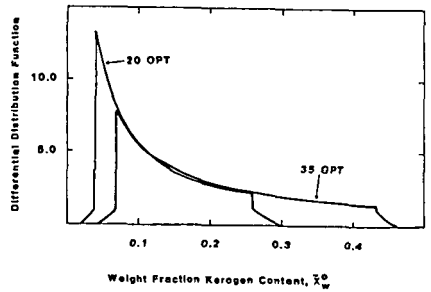


Figure 10
AREA NORMALIZED HISTOGRAM OF
WEIGHT FRACTION KEROGEN FOR SHALE D

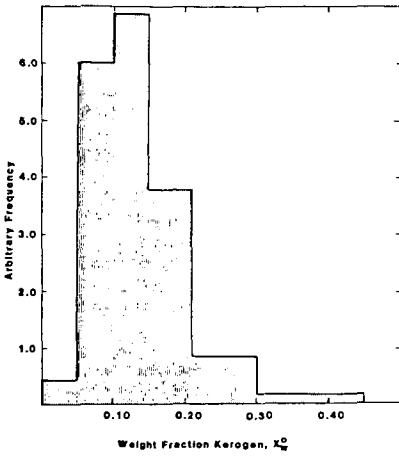


Figure 11
PREDICTED DIFFERENTIAL DISTRIBUTION
FOR 20.6 GPT ($\bar{x}_w^0 = 0.12$) SHALE

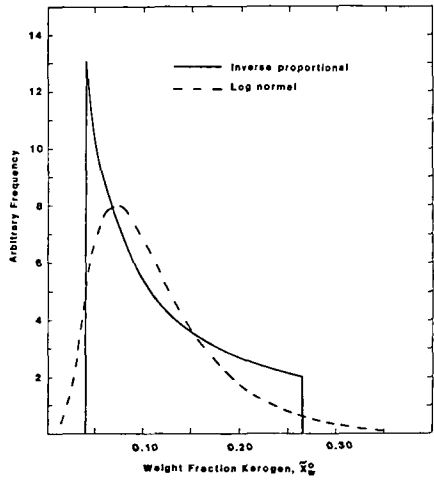


Figure 12
PREDICTED ENRICHMENT PLOT FOR 20.6 GPT ($\bar{x}_w^0 = 0.12$) SHALE

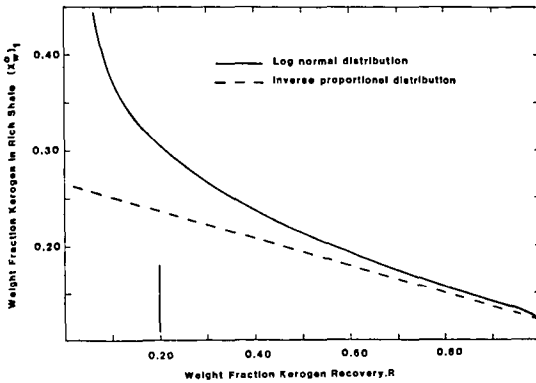


Figure 13
CUMULATIVE WEIGHT FRACTION DISTRIBUTION
CURVE FOR SHALE AS A FUNCTION OF WEIGHT
FRACTION KEROGEN

